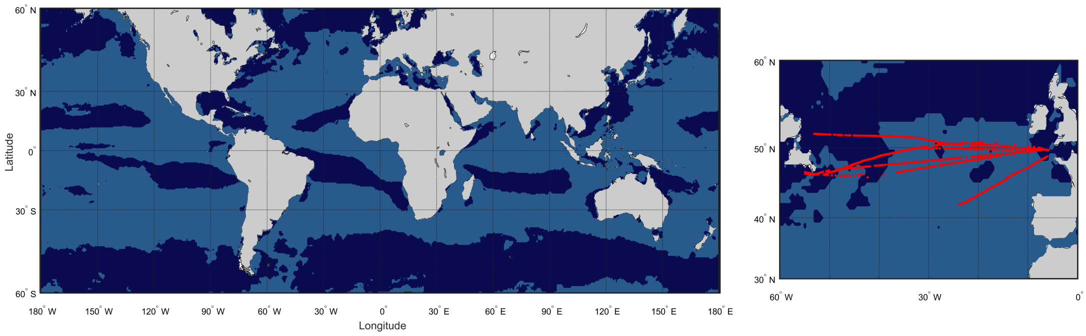

(a) Sea state conditions from September to December 2007

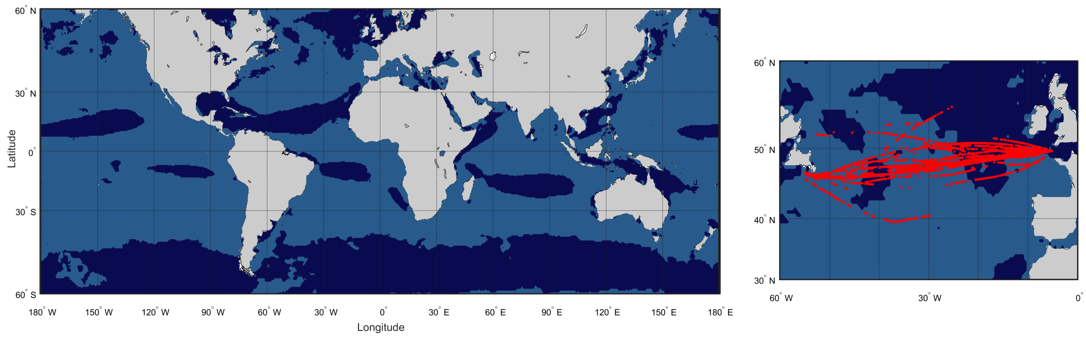

(b) Sea state conditions from January to December 2008

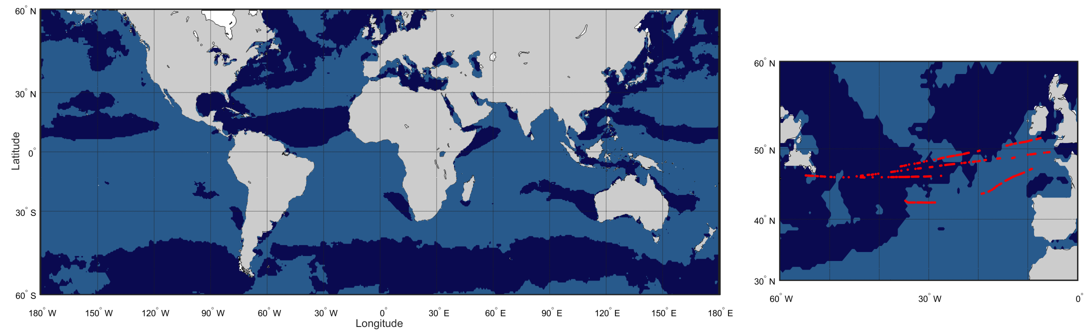

(c) Sea state conditions from January to March 2009

Figure 6.11: Geographical distribution of predominant unimodal and bimodal sea state conditions.

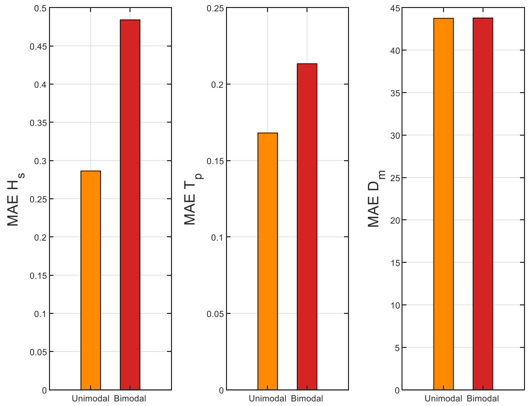

(a) Estimated sea state parameters – wave radar

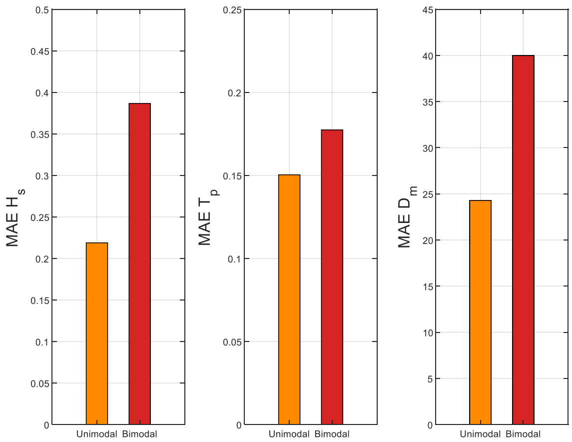

(b) Estimated sea state parameters – ERA5

Figure 6.12: MAEs comparison between unimodal and bimodal sea state reconstructions.

Chapter 7

Results: Bimodal sea state conditions

This Chapter presents the validation of the numerical procedure for bimodal sea state condition outlied in Chapter 5. The algorithm is validated by synthetic ship motion dataset as detailed in the following.

7.1 Benchmark study

The wind sea and swell prevailing directions range from 0 up to 360°, with 10° step, so obtaining a total number of 1081 simulations, with 1-h duration lying in Area I of Figure 5.3. The remaining sea state parameters have been varied as detailed in Table 5.1. Figures 7.1 depicts the simulated versus the estimated equivalent sea state parameters, namely: (i) the compass angle of the prevailing wave direction, (ii) the significant wave height and (iii) the wave energy period of the equivalent sea state. The MAE on the equivalent prevailing wave direction is equal to 7.030 deg, while the MAEs on the equivalent significant wave height and wave energy period are equal to 8.6% and 6.4%, respectively. It is noticed that in Figure 7.1 (b) the scatter between the estimated and simulated data increases among with the significant wave height. On the contrary, the relative Absolute Error (AE) remains almost constant, proving that the reliability of the algorithm is independent of the significant wave height value.
Subsequently, an additional analysis can be carried out, by reducing the time history length. Hence, Table 7.1 provides the MAEs corresponding to 30 and 15 min, together with the percentage increase, as regards the 1-h reference values. As predictable, the MAEs increase with the decrease of the updating time interval. Particularly, the MAEs increase by about 10% if the time interval is reduced from 60 to 30 min. If it further decreases up to 15 min, the MAE on the equivalent significant wave height raises up to 45%, so becoming no more acceptable. Hence, a time interval equal to 30 min seems to be a good choice to contemporarily ensure a good accuracy of the algorithm and a fast updating of sea state parameters.

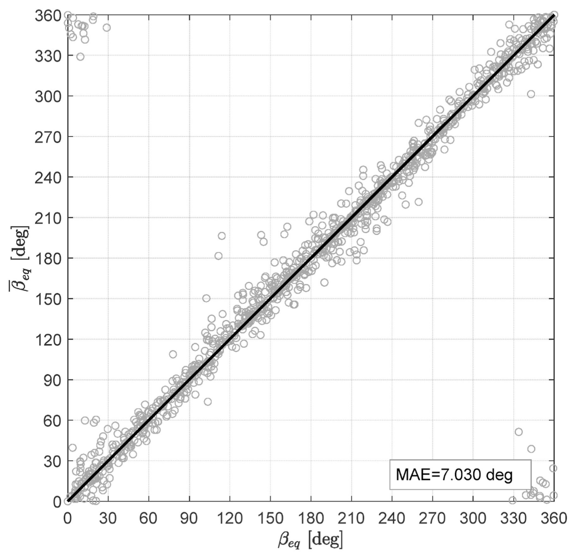

(a) Equivalent prevailing direction

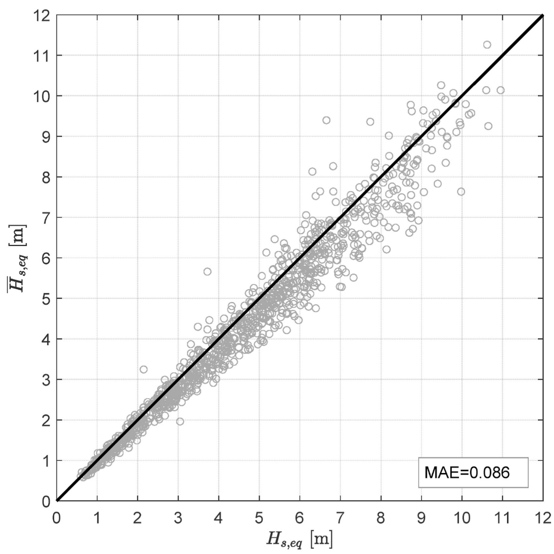

(b) Equivalent significant wave height

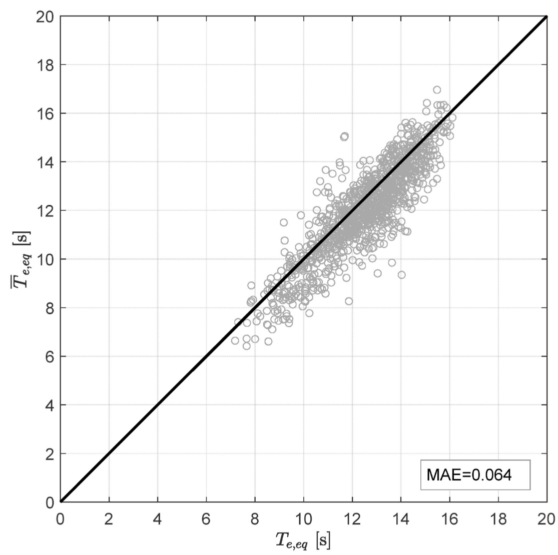

(c) Equivalent wave energy period

Figure 7.1: Benchmark study – Time length = 60 min.

Time duration [min]	60	30	15	Δ_{30-60} [%]	Δ_{15-60} [%]
MAE β_{eq} [deg]	7.030	7.730	8.318	9.957	18.321
MAE $H_{s,\text{eq}}$ [—]	0.086	0.094	0.124	9.302	44.186
MAE $T_{e,\text{eq}}$ [—]	0.064	0.072	0.082	12.500	28.125

Table 7.1: MAEs as a function of time interval.

7.2 Statistics of errors

Finally, Figure 7.2 provides the probability density functions (pdfs) of the Absolute Errors (AEs), together with the relevant best-fit exponential distributions. In all cases, the bin width of the normalised frequency histograms is selected by the Freedman and Diaconis (1981) rule. By Figure 7.2(a) it is gathered that the AE on the equivalent prevailing direction is generally lower than 20 degs, with most of the data less than 10 degs. As concerns the remaining sea state parameters, the AE is generally lower than 0.20, with most of the data less than 0.10. These results confirm that the accuracy of the algorithm in Area I of Figure 5.3 is very high. This outcome is also proved by Table **??**, that provides the quantiles Q_p of the best-fit exponential distributions at various percentile levels, from which it is also gathered that the AEs on the equivalent sea state parameters are widely acceptable up to the 90^{th} percentile of the relevant distributions.

Percentile	0.50	0.75	0.90	0.95	0.99
$Q_p(\beta_{eq})$ [deg]	5.358	10.716	17.798	23.156	35.597
$Q_p(H_{s,eq})$ [–]	0.065	0.130	0.216	0.281	0.432
$Q_p(T_{e,eq})$ [–]	0.050	0.100	0.166	0.216	0.332

Table 7.2: Statistics of errors – percentiles of the equivalent sea state parameters.

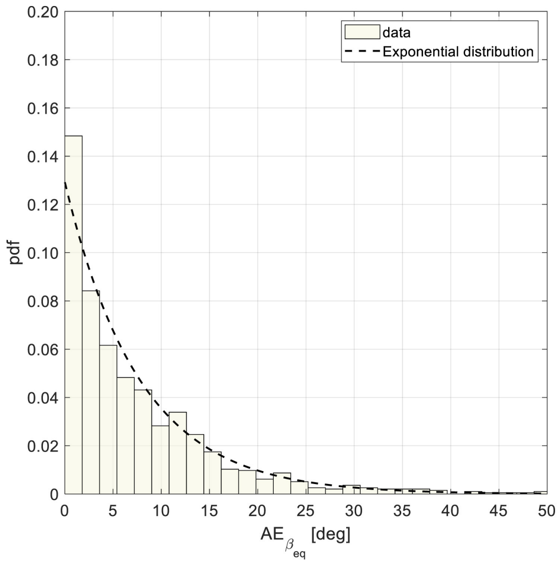

(a) Equivalent prevailing direction

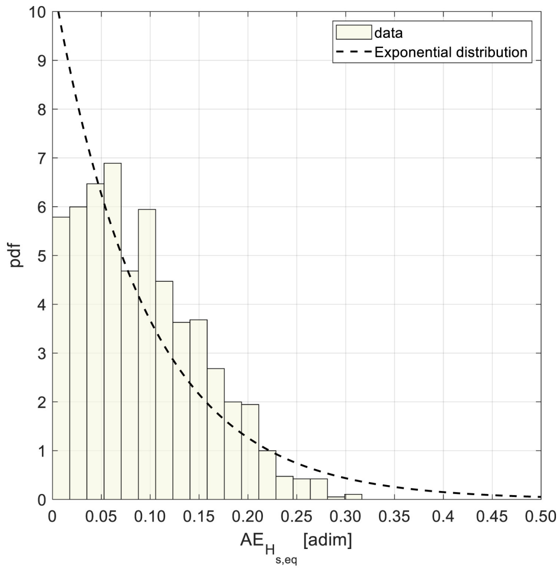

(b) Equivalent significant wave height

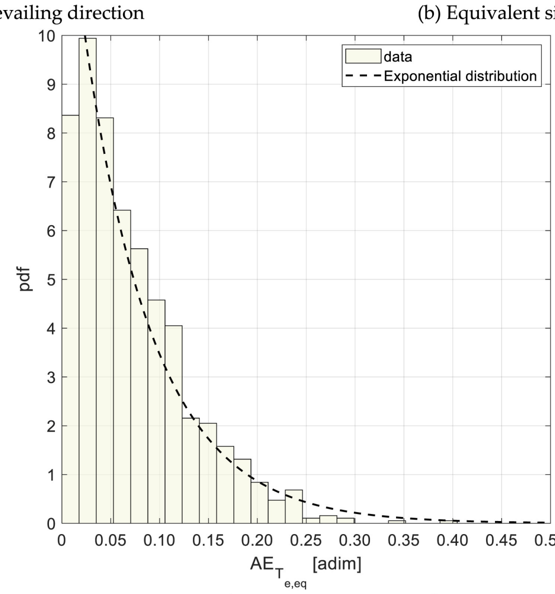

(c) Equivalent wave energy period

Figure 7.2: Statistics of errors – Time length = 30 min

Chapter 8

Conclusions and Future works

This Chapter outlines the main findings achieved in this thesis and provides some insights for future research.

8.1 Summary of the main findings

The main objective of the present study was to develop numerical methods for the measurement of sea state parameters on the basis of the ship motion analysis. Starting from the literature review on existing methods, two novel parametric procedures were developed to estimate unimodal and bimodal short-crested sea state condition. The performance and the applicability of the developed methodologies throughout this PhD thesis were tested through multiple case studies, making use of synthetic and full-scale data. The flowchart in Figure 8.1 provides a logical scheme of the procedures developed for estimating sea state conditions. The process starts with the data ingestion of ship motion measurements and hydrodynamic data, followed by a data processing phase in which the sea state is classified as unimodal or bimodal. In the former case, the sea state estimation is outlined using the numerical procedure described in Chapter 4, whereas in the latter case the procedure detailed in Chapter 5 is adopted. For bimodal sea states, an additional signal processing step is applied to separate wind sea and swell components using the filters defined in Equations (5.2) and (5.3). As previously mentioned, the optimization phase is based on the correlation between measured and tentative spectra, which is evaluated using Spearman and Pearson correlation coefficients according to Equations (4.14) and (4.22). As a final step, the main wave parameters are estimated.

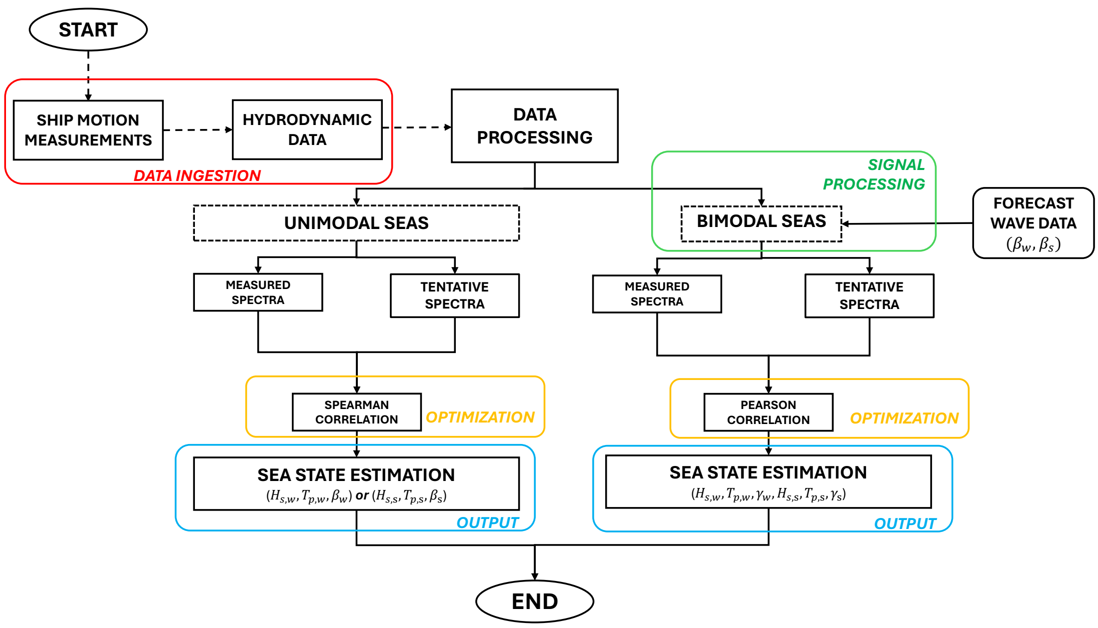

Figure 8.1: Logical sequence of the developed procedures.

As concerns the level of accuracy for the validation tests carried out using the unimodal procedure developed in Chapter 4, it can be summarized as follows. The performance of the algorithm, for unimodal sea state condition has been tested in terms of Mean Absolute Errors by varying the heading angle from 0 to 180 deg with 30 deg step. The maximum MAE on the significant wave height is equal to 3% at 60 deg, while the maximum error on the wave peak period is equal to 3% and occur at 0 deg. The worst estimation performance for both parameters corresponds to the following sea conditions. The same trend is confirmed for the heading angle, where the maximum MAE equal to 2.9 deg occurs at following seas.
The error increases if the algorithm is applied to real ship motion data. Nevertheless, some uncertainties mainly related to the knowledge of some parameters affecting the reliability of the method, such as the ship loading conditions and the draught do not allow to make reliable conclusions with reference to the employment in a real scenario. As concerns the bimodal numerical procedure outlined in Section 5, the sea state reconstruction algorithm accurately estimates sea state parameters in about the 83% of bimodal sea state conditions considering all possible combinations of heading angles due to the wind sea and swell components, with the only exception of case lying in Area II of Figure 5.3. Moreover, the 30 min time interval has been identified as the most suitable compromise to ensure a high reliability of the algorithm combined with a fast updating of sea state parameters. In this respect, the error on the equivalent heading angle at the 90^{th} percentile is equal to 17.8 degs, while those one relative to the significant wave height and wave peak period are equal to 21.6% and 16.6%, respectively. These findings highlight the advantage of combining the data relative to the wind and swell prevailing directions provided by external sources, such as the ECMWF forecast one, with the wave buoy analogy method that allows estimating all the remaining sea

state parameters. The outcomes of this PhD project contribute to the C-MOST project that financially supported this research. Particularly, this research pertains to the SPOKE 3 at the work packages 'Toward Autonomous Navigation' and 'Digital Twin Technologies'.

8.2 Future work

The main outcomes achieved were addressed by considering a limited number of case studies and scenarios. The main limitation of this research is the issue of testing in real scenarios. Even though the author declares that most of the conclusions have validity, the need for future work in terms of investigating more cases is undeniable. As concerns the developed numerical procedures, it should be noted that the unimodal procedure was validated using both synthetic and full-scale data, collected on-board a containership, whereas the bimodal model was validated only based on synthetic ship-motion datasets. However, in the middle of July 2025, a test was also conducted at the Lake of Nemi (RM). Such experimental campaign provided the opportunity to test the hardware configuration developed for measuring ship responses even if this topic was out the goals of the PhD research activities. In this respect, Figure 8.2 depict the RIB employed during the experiments and the trajectory followed around the lake.

Before the lake tests, a dedicated hardware system was designed and tested for future ship-

(a) Experimental test at the Lake of Nemi.

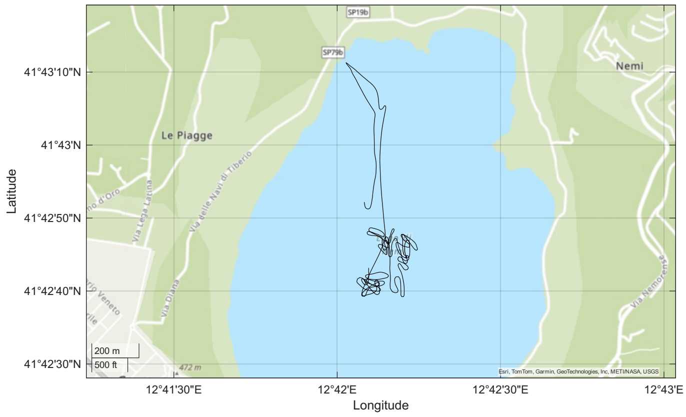

(b) Course around Lake of Nemi.

Figure 8.2: Views of Lake Nemi.

board installation. The system integrates a Raspberry Pi 5 with a low-cost GNSS/INS receiver (U-Blox C102-F9R). Specifically, the Raspberry Pi handles synchronisation of data streams, logging and data transmission to the laboratory server, while the U-Blox C102-F9R was selected for its advanced positioning accuracy and integrated Inertial Navigation System (INS). This combination enables continuous estimation of vessel position and attitude, even in case of temporary GNSS signal loss. For these purposes, a key advantage of the ZED-F9R module is the built-in 6-axis IMU (Inertial Measurement Unit), which allows the implementation of sophisticated sensor fusion approaches.

These devices were positioned on the RIB, with the GNSS antenna fixed at the bow and the Raspberry Pi and U-Blox mounted inside a bow locker, as shown in Figure 8.3. The entire setup was designed in cooperation with the Parthenope PANG Research group to support applications requiring reliable navigation and accurate position and attitude tracking. The system was designed to operate autonomously onboard a vessel, collecting and sending motion and positioning data to a web server to estimate sea state parameters. Based on those remarks, possible future works include the testing phase of the developed algorithm in a more complex scenario including possible errors in the assessment of the ship transfer functions, as well as further extension of the method to multi-peaked wave spectra and hybrid approaches that investigate frequency-domain model with data-driven algorithm. Those topics will be the subject of future research.

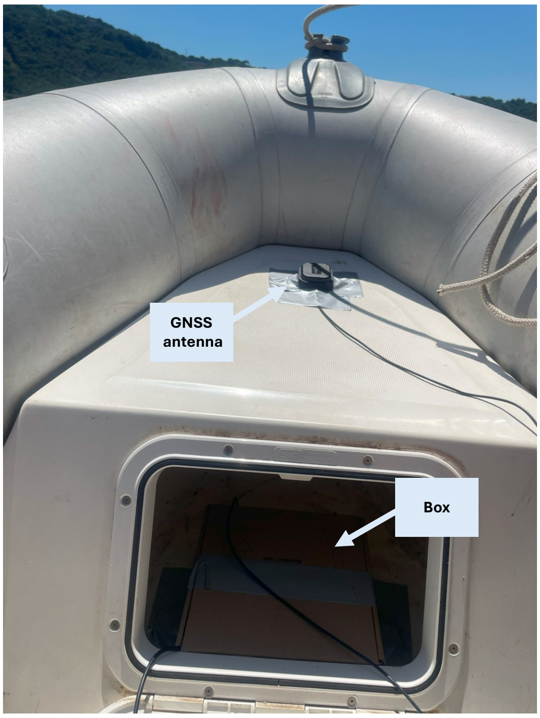

Figure 8.3: RIB bow with a GNSS antenna mounted on top and a box stored in the bow locker.

Bibliography

Airy, G. B. (1845). *Tides and waves*. Extracted from the Enciclopedia Metropolitana.

Ardhuin, F., Stopa, J. E., Chapron, B., Collard, F., Husson, R., Jensen, R. E., Johannessen, J., Mouche, A., Passaro, M., Quartly, G. D., et al. (2019). Observing sea states. *Frontiers in Marine Science*, *6*, 124.

Ascione, S., Nielsen, U., Piscopo, V., & Storhaug, G. (2026). Sea state reconstruction based on the spearman rank correlation using full-scale data from a containership. *Ocean Engineering*, *343*, 123471.

Ascione, S., Piscopo, V., & Scamardella, A. (2024). Comparison of linear and rank-correlation for the sea state estimation. *Proceedings of the 2024 IEEE International Workshop on Metrology for the Sea; Learning to Measure Sea Health Parameters (MetroSea), Portorož, Slovenia, 14–16 October 2024*, 250–255.

Babarit, A., & Delhommeau, G. (2015). Theoretical and numerical aspects of the open source bem solver nemoh. *Proceedings of the 11th European wave and tidal energy conference, Madeira, Portugal, 11th September 2025.*

Booij, N., Ris, R. C., & Holthuijsen, L. H. (1999). A third-generation wave model for coastal regions: Model description and validation. *Journal of geophysical research: Oceans*, *104*(C4), 7649–7666.

Bretschneider, C. L. (1959). *Wave variability and wave spectra for wind-generated gravity waves* (tech. rep. No. 118). Beach erosion board corps of engineers.

Butsanets, A., Karetnikov, V., & Ol'Khovik, E. (2021). Overview of test water areas for testing unmanned and autonomous vessels. *International Scientific Siberian Transport Forum*, 1474–1482.

Chakrabarti, S. K. (2005). Handbook of offshore engineering. *Offshore Structure Analysis, Inc. Plainfield, Illinois, USA*, *1*, 79.

Cummins, W. (1962). The impulse response function and ship motions. *Schiffstechnik*, *47*, 1–29.

Dijkstra, E. W. (1959). A note on two problems in connexion with graphs. *Numerische mathematik*, *1*(1), 269–271.

DNV. (2000). *Environmental conditions and environmental loads*. Det Norske Veritas Oslo, Norway.

DNV. (2010). *Environmental conditions and environmental loads: Recommended practice DNV-RP-C205* (tech. rep. No. DNV-RP-C205). Det Norske Veritas. Høvik, Norway.

DNV. (2017). *Recommended practice DNVGL-RP-C205 environmental conditions and environmental loads* (tech. rep.). Det Norske Veritas.

Elsevier. (2024). Scopus Database [Accessed: 7 June 2025].

Ergin, A., Alley, E., Brandt, A., Drummen, I., Hermundstad, O., Huh, Y. C., Ivaldi, A., Liu, J. H., Malenica, S., el Moctar, O., Shyu, R. J., Storhaug, G., Vladimir, N., Yamada, Y., Zhan, D., & Zhang, G. (2018). Committee ii.2: Dynamic response. *Proceedings of the International Ship and Offshore Structures Congress (ISSC)*, 255–333.

Evensen, M. H. (2020). *Safety and security of autonomous vessels. based on the yara birkeland project* [Master's thesis, The University of Bergen].

Fisher, R. A. (1921). On the" probable error" of a coefficient of correlation deduced from a small sample. *Metron*, *1*, 3–32.

Freedman, D., & Diaconis, P. (1981). On the histogram as a density estimator: L 2 theory. *Zeitschrift für Wahrscheinlichkeitstheorie und verwandte Gebiete*, *57*(4), 453–476.

Gibbons, J. D. (1985). Nonparametric statistical inference. *Revised and Expanded, second ed. Marcel Dekker Inc.*

Gledić, I., Petranović, T., Katalinić, M., Vujičić, S., Matić, P., Ćatipović, I., & Parunov, J. (2022). Comparison of full-scale measurements and seakeeping calculations for two research vessels in the adriatic sea. *Ocean engineering*, *266(113135)*.

Goda, Y. (2010). *Random seas and design of maritime structures*. World Scientific.

González, M., Uriarte, A., Fontán, A., Mader, J., & Gyssels, P. (2004). Marine dynamics. In *Elsevier oceanography series* (pp. 133–157, Vol. 70). Elsevier.

Hasselmann, D. E., Dunckel, M., & Ewing, J. (1980). Directional wave spectra observed during JONSWAP 1973. *Journal of Physical Oceanography*, *10*(8), 1264–1280.

Håvold, J. I. (2005). Safety-culture in a norwegian shipping company. *Journal of safety research*, *36*(5), 441–458.

Hersbach, H., Bell, B., Berrisford, P., Hirahara, S., Horányi, A., Muñoz-Sabater, J., Nicolas, J., Peubey, C., Radu, R., Schepers, D., et al. (2020). The ERA5 global reanalysis. *Quarterly journal of the royal meteorological society*, *146*(730), 1999–2049.

Hua, J., & Palmquist, M. (1994). Wave estimation through ship motion measurement. *KTH Royal Institute of Technology, Department of Aeronautical and Vehicle Engineering, Centre for Naval Architecture, Stockholm, Sweden*.

Huss, M., & Olander, A. (1994). *Theoretical seakeeping predictions on board ships: A system for operational guidance and real time surveillance*. Naval Architecture, Department of Vehicle Engineering, Royal Inst. of Technology.

IMO. (2008). Casualty Investigation Code (Resolution MSC.255(84)) [Accessed: 2025-06-07].

IMO. (2019). *MSC.1/circ.1604 – interim guidelines for maritime autonomous surface ships (MASS) trials* [MSC.1/Circ.1604].

Iseki, T., & Nielsen, U. D. (2015). Study on short-term variability of ship responses in waves. *The Journal of Japan Institute of Navigation*, *132*, 51–57.

Iseki, T., & Ohtsu, K. (2000). Bayesian estimation of directional wave spectra based on ship motions. *Control Engineering Practice*, *8*(2), 215–219.

Isobe, M., Kondo, H., & Horikawa, K. (1984). Expansion of MLM for estimation of directional spectra". *Proceedings of the Coastal Engineering, JSCE*, *31*, 173–177.

James, R. W. (1975). *Application of wave forecasts to marine navigation* (tech. rep.). U.S. Naval Oceanographic Office. Washington, D.C.

Kawai, T., Kawamura, Y., Okada, T., Mitsuyuki, T., & Chen, X. (2021). Sea state estimation using monitoring data by convolutional neural network (CNN). *Journal of Marine Science and Technology*, *26*(3), 947–962.

Kim, M., Hizir, O., Turan, O., Day, S., & Incecik, A. (2017). Estimation of added resistance and ship speed loss in a seaway. *Ocean Engineering*, *141*, 465–476.

Kim, T., Lin, L.-H., & Wang, H. (1995). Application of maximum entropy method to the real sea data. *Coastal Engineering 1994*, 340–355.

Kobune, K., & Hashimoto, N. (1986). Estimation of directional spectra from the maximum entropy principle. *International offshore mechanics and arctic engineering. Symposium. 5*, 80–85.

Komen, G. J., Cavaleri, L., Donelan, M., Hasselmann, K., Hasselmann, S., & Janssen, P. (1996). *Dynamics and modelling of ocean waves*. Cambridge University Press.

Kong, W., Lam, C.-c., Lau, D.-s., Chow, C.-k., Chong, S.-n., Chan, P.-w., & Leung, N.-c. (2024). Model validation and applications of wave and current forecasts from the hong kong observatory's operational marine forecasting system. *Ocean Modelling*, *190(102393)*, 1–29.

Lewis, E., of Naval Architects, S., & (U.S.), M. E. (1988). *Principles of naval architecture*. Society of Naval Architects; Marine Engineers.

Lindemann, K., Odland, J., & Strengtheagen, J. (1977). *On the application of hull surveillance systems for increased safety and improved structural utilization in rough weather* (tech. rep.). Society of Naval Architects and Marine Engineers.

Luo, M., & Shin, S.-H. (2019). Half-century research developments in maritime accidents: Future directions. *Accident Analysis & Prevention*, *123*, 448–460.

Majidian, H., Wang, L., & Enshaei, H. (2022). Part.A: A review of the real-time sea-state estimation, using wave buoy analogy. *Ocean Engineering*, *266(111684)*.

Majidiyan, H., Enshaei, H., Howe, D., & Wang, Y. (2024). An integrated framework for real-time sea-state estimation of stationary marine units using wave buoy analogy. *Journal of Marine Science and Engineering*, *12*(12).

Mansard, E., & Funke, E. (1991). On the fitting of jonswap spectra to measured sea states. *Coastal Engineering*, 464–477.

Mansouri, S. A., Lee, H., & Aluko, O. (2015). Multi-objective decision support to enhance environmental sustainability in maritime shipping: A review and future directions. *Transportation Research Part E: Logistics and Transportation Review*, *78*, 3–18.

MathWorks. (2024). Cross power spectral density - cpsd function [Accessed: 2024-03-05]. https://it.mathworks.com/help/signal/ref/cpsd.html

Michel, W. H., et al. (1968). Sea spectra simplified. *Marine Technology*, *5*(1), 17–30.

Michel, W. H., et al. (1999). Sea spectra revisited. *Mar Technol*, *36*(4), 211–227.

Mittendorf, M., Nielsen, U. D., Bingham, H. B., & Storhaug, G. (2022). Sea state identification using machine learning—a comparative study based on in-service data from a container vessel. *Marine Structures*, *85(103274)*.

Montazeri, N., Nielsen, U. D., & Jensen, J. J. (2016). Estimation of wind sea and swell using shipboard measurements–a refined parametric modelling approach. *Applied Ocean Research*, *54*, 73–86.

Moskowitz, L. (1964). Estimates of the power spectrums for fully developed seas for wind speeds of 20 to 40 knots. *Journal of geophysical research*, *69*(24), 5161–5179.

Mounet, R. E. G. (2023). *Sea state estimation based on measurements from multiple observation platforms* [Doctoral dissertation, Technical University of Denmark].

Nestegård, A., Ronæss, M., Hagen, Ø., Ronold, K. O., & Bitner-Gregersen, E. (2006). New DNV recommended practice DNV-RP-C205 on environmental conditions and environmental loads. *Proceedings of the Sixteenth (2006) International Offshore and Polar Engineering Conference, San Francisco, California, USA, 28 May- 2 June*.

Nielsen, U. D., Bingham, H. B., Brodtkorb, A. H., Iseki, T., Jensen, J. J., Mittendorf, M., Mounet, R. E., Shao, Y., Storhaug, G., Sørensen, A. J., et al. (2023). Estimating waves via measured ship responses. *Scientific Reports*, *13*(1).

Nielsen, U. D., Bjerregård, M., Galeazzi, R., & Fossen, T. I. (2015). New concepts for shipboard sea state estimation. *Proceedings of the OCEANS 2015-MTS/IEEE Washington, USA, 19-22 October 2015*, 1–10.

Nielsen, U. D., Brodtkorb, A. H., & Sørensen, A. J. (2019). Sea state estimation using multiple ships simultaneously as sailing wave buoys. *Applied Ocean Research*, *83*, 65–76.

Nielsen, U. D., Iwase, K., & Mounet, R. E. (2024). Comparing machine learning-based sea state estimates by the wave buoy analogy. *Applied Ocean Research*, *149(104042)*.

Nielsen, U. D., & Stredulinsky, D. C. (2012). Sea state estimation from an advancing ship–a comparative study using sea trial data. *Applied Ocean Research*, *34*, 33–44.

Nielsen, U. D. (2006). Estimations of on-site directional wave spectra from measured ship responses. *Marine Structures*, *19*(1), 33–69.

Nielsen, U. D. (2007). Response-based estimation of sea state parameters—influence of filtering. *Ocean Engineering*, *34*(13), 1797–1810.

Nielsen, U. D. (2017). A concise account of techniques available for shipboard sea state estimation. *Ocean Engineering*, *129*, 352–362.

Pascoal, R., Perera, L. P., & Soares, C. G. (2017). Estimation of directional sea spectra from ship motions in sea trials. *Ocean Engineering*, *132*, 126–137.

Pascoal, R., & Soares, C. G. (2009). Kalman filtering of vessel motions for ocean wave directional spectrum estimation. *Ocean Engineering*, *36*(6-7), 477–488.

Pawlowski, M. (2011). Sea spectra revisited. *Contemporary Ideas on Ship Stability and Capsizing in Waves*, 573–587.

Pennino, S., Gaglione, S., Innac, A., Piscopo, V., & Scamardella, A. (2020). Development of a new ship adaptive weather routing model based on seakeeping analysis and optimization. *Journal of Marine Science and Engineering*, *8*(4), 270.

Piscopo, V., Ascione, S., & Scamardella, A. (2025). Assessment of bimodal sea states by the wave buoy analogy method. *Ocean Engineering*, *340(122258)*.

Piscopo, V., Scamardella, A., & Gaglione, S. (2020). A new wave spectrum resembling procedure based on ship motion analysis. *Ocean Engineering*, *201(107137)*.

Piscopo, V., Ascione, S., & Scamardella, A. (2024). A new wave spectrum assessment procedure based on spearman rank correlation algorithm. *Ocean Engineering*, *308(118348)*.

Rossi, G. B., Cannata, A., Iengo, A., Migliaccio, M., Nardone, G., Piscopo, V., & Zambianchi, E. (2021). Measurement of sea waves. *Sensors*, *22*(1), 78.

Salvesen, N., Tuck, E., & Faltinsen, O. (1970). Ship motions and sea loads. *Proceedings of the Society of Naval Architects and Marine Engineers New York, 12-13 November 1970*.

Sedgwick, P. (2012). Pearson's correlation coefficient. *Bmj*, *345*.

Skoglund, L. (2012). *A new method for robust route optimization in ensemble weather forecasts* (Report, Physics / Aeronautical and Vehicle Engineering, Naval Systems). KTH, School of Engineering Sciences (SCI).

Stammer, D., & Chassignet, E. (2000). Ocean state estimation and prediction in support of oceanographic research. *Oceanography*, *13*(2), 51–56.

Stansberg, C., Contento, G., Hong, S. W., Irani, M., Ishida, S., Mercier, R., Wang, Y., Wolfram, J., Chaplin, J., & Kriebel, D. (2002). The specialist committee on waves final report and recommendations to the 23rd ITTC. *Proceedings of the 23rd ITTC,Venice, Italy*, *2*, 505–551.

Storhaug, G. (2007). Measurements of wave induced vibrations onboard a large container vessel operating in harsh environment. *Proceedings of the 10th international symposium on practical design of ships and other floating structures, Houston, US, 30 September - 5 October 2007*, *1*, 64–72.

Takekuma, K., & Takahashi, T. (1973). On the evalution of sea spectra based on the measured ship motions. *Transactions of the West-Japan Society of Naval Architects*, (45), 51–57.

Tolman, H. L., Balasubramaniyan, B., Burroughs, L. D., Chalikov, D. V., Chao, Y. Y., Chen, H. S., & Gerald, V. M. (2002). Development and implementation of wind-generated ocean surface wave modelsat NCEP. *Weather and forecasting*, *17*(2), 311–333.

Tu, F., Ge, S. S., Choo, Y. S., & Hang, C. C. (2018). Sea state identification based on vessel motion response learning via multi-layer classifiers. *Ocean Engineering*, *147*, 318–332.

Zago, L., Simos, A. N., Kawano, A., & Kogishi, A. M. (2023). A new vessel motion based method for parametric estimation of the waves encountered by the ship in a seaway. *Applied Ocean Research*, *134(103499)*.

Zoppoli, R. (1972). Minimum-time routing as an n-stage decision process. *Journal of Applied Meteorology*, 429–435.